Journal of Experimental Botany
doi:10.1093/jxb/erab127 Advance Access Publication 19 March, 2021
This paper is available online free of all access charges (see https://academic.oup.com/jxb/pages/openaccess for further details)

RESEARCH PAPER

A meta-analysis of mesophyll conductance to CO_2 in relation to major abiotic stresses in poplar species

Raed Elferjani[1,*], Lahcen Benomar[2,*,†], Mina Momayyezi[3], Roberto Tognetti[4], Ülo Niinemets[5], Raju Y. Soolanayakanahally[6], Guillaume Théroux-Rancourt[7], Tiina Tosens[5], Francesco Ripullone[8], Simon Bilodeau-Gauthier[9], Mohammed S. Lamhamedi[9], Carlo Calfapietra[10] and Mebarek Lamara[2]

[1] Quebec Network for Reforestation and Intensive Silviculture, TELUQ University, Montreal, QC, H2S 3L5, Canada
[2] Forest Research Institute, University of Quebec in Abitibi-Temiscamingue, Rouyn-Noranda, QC, J9X 5E4, Canada
[3] Department of Viticulture and Enology, University of California, Davis, CA 95616, USA
[4] Università degli Studi del Molise, Via De Sanctis, 86100 Campobasso, Italy
[5] Estonian University of Life Sciences, Kreutzwaldi 1, 51006 Tartu, Estonia
[6] Indian Head Research Farm, Agriculture and Agri-Food Canada, Indian Head, SK, S0G 2K0, Canada
[7] Institute of Botany, University of Natural Resources and Life Sciences, Gregor-Mendel-Strasse 33, 1180 Vienna, Austria
[8] University of Basilicata, Via Ateneo Lucano 10, 85100 Potenza, Italy
[9] Direction de la Recherche Forestière, 2700 rue Einstein, Québec, QC, G1P 3W8, Canada
[10] Institute of Agro-Environmental & Forest Biology (IBAF), National Research Council (CNR), Via Marconi 2, Porano (TR) 05010, Italy

* These authors contributed equally to this work.
† Correspondence: lahcen.benomar.1@gmail.com

Received 8 December 2020; Editorial decision 15 March 2021; Accepted 17 March 2021

Editor: Ros Gleadow, Monash University, Australia

Abstract

Mesophyll conductance (g_m) determines the diffusion of CO_2 from the substomatal cavities to the site of carboxylation in the chloroplasts and represents a critical component of the diffusive limitation of photosynthesis. In this study, we evaluated the average effect sizes of different environmental constraints on g_m in *Populus* spp., a forest tree model. We collected raw data of 815 A–C_i response curves from 26 datasets to estimate g_m, using a single curve-fitting method to alleviate method-related bias. We performed a meta-analysis to assess the effects of different abiotic stresses on g_m. We found a significant increase in g_m from the bottom to the top of the canopy that was concomitant with the increase of maximum rate of carboxylation and light-saturated photosynthetic rate (A_{max}). g_m was positively associated with increases in soil moisture and nutrient availability, but was insensitive to increasing soil copper concentration and did not vary with atmospheric CO_2 concentration. Our results showed that g_m was strongly related to A_{max} and to a lesser extent to stomatal conductance (g_s). Moreover, a negative exponential relationship was obtained between g_m and specific leaf area, which may be used to scale-up g_m within the canopy.

Keywords: Abiotic stress, A–C_i curve, mesophyll conductance, meta-analysis, photosynthesis, poplar.

Introduction

Carbon assimilation in plants is importantly determined by the diffusion efficiency of CO_2 from the atmosphere to the site of carboxylation. The rate of CO_2 diffusion is affected by two main diffusion limitations. The first limitation controls the CO_2 flux from the atmosphere to the sub-stomatal cavities through the stomata and is characterized by stomatal conductance (g_s). The second limitation determines the diffusion of CO_2 from the substomatal cavities to the sites of carboxylation in the chloroplasts and is characterized by mesophyll conductance (g_m). g_m is composed of gaseous and liquid phase resistances (Flexas *et al.*, 2008; Evans *et al.*, 2009; Niinemets *et al.*, 2009). CO_2 diffusion inside the leaves is complex, facing a series of structural barriers coupled with biochemical regulation. It has been shown that g_m is typically limited by liquid phase conductance both in species with soft mesophytic leaves and in species with tough xerophytic leaves (Tosens *et al.*, 2012*a*, *b*; Tomás *et al.*, 2013). The liquid phase is a multicomponent pathway that involves the mesophyll cell wall thickness and porosity, the plasmalemma, the chloroplast envelope, the chloroplast thickness, and the mesophyll surface area exposed to intercellular air spaces per unit of leaf area (Evans *et al.*, 2009; Tosens *et al.*, 2012*b*; Tomás *et al.*, 2013). After extensive study during the past two decades, g_m is now widely accepted as a critical limiting factor to photosynthesis, which has to be considered in characterizing plant carbon gain potentials and responses to future climate change (Evans *et al.*, 2009; Niinemets *et al.*, 2009, 2011; Flexas *et al.*, 2016).

Mesophyll conductance has been shown to respond to environmental stress and may govern functional plasticity of photosynthesis and plant fitness under limited resources (Galle *et al.*, 2009; Barbour *et al.*, 2010; Buckley and Warren, 2014; Théroux Rancourt *et al.*, 2015; Flexas *et al.*, 2016; Shrestha *et al.*, 2018). However, recent findings on the response of g_m to abiotic stress are conflicting and inconclusive, demonstrating the complex nature of g_m variation (Flexas *et al.*, 2008; Niinemets *et al.*, 2009; Zhou *et al.*, 2014; Shrestha *et al.*, 2018). This suggests that the environmental and species-specific responses (and consequently the level of acclimation) of g_m to growth conditions should be considered in predicting plant performance in the field. Among the contrasting environmental responses, growth temperature may (Warren, 2008; Silim *et al.*, 2010) or may not (Dillaway and Kruger, 2010; Benomar *et al.*, 2018) affect g_m. Similarly, the increase in soil nitrogen may (Warren, 2004; Shrestha *et al.*, 2018; Xu *et al.*, 2020; Zhu *et al.*, 2020) or may not (Bown *et al.*, 2009) stimulate g_m. The magnitude of decrease in g_m under water stress and low light differed among studies (Warren *et al.*, 2003; Niinemets *et al.*, 2006; Montpied *et al.*, 2009; Bögelein *et al.*, 2012; Tosens *et al.*, 2012*a*; Zhou *et al.*, 2014; Peguero-Pina *et al.*, 2015; Théroux Rancourt *et al.*, 2015). These discrepancies among studies result in part from (i) the absolute changes in structural and biochemical traits controlling g_m, as well as from changes in the relative contribution of these traits (Marchi *et al.*, 2008; Tomás *et al.*, 2013), and (ii) the level of coordination between g_m, g_s, and leaf specific hydraulic conductivity (K_L) (Flexas *et al.*, 2013; Théroux-Rancourt *et al.*, 2014; Xiong *et al.*, 2017). Given the complex interplay between different factors controlling g_m, it is important to examine its acclimation at the genus and species level to gain a general insight into the mechanistic basis of changes in g_m.

Five methods exist to estimate g_m: (i) chlorophyll fluorescence coupled to gas exchange (Harley *et al.*, 1992), (ii) carbon isotope discrimination coupled to gas exchange (initially developed by Evans *et al.*, 1986), (iii) oxygen isotope discrimination (Barbour *et al.*, 2016), (iv) A–C_i curve fitting (Ethier and Livingston, 2004; Sharkey *et al.*, 2007), and (v) 1D modeling of g_m from leaf structural characteristics (Evans *et al.*, 2009; Tosens *et al.*, 2012*b*; Tomás *et al.*, 2013). All of these methods are based on specific assumptions and each one has its limitations (Flexas *et al.*, 2013; Tosens and Laanisto, 2018). The standard deviation of the estimate of g_m may vary from 10% to 40%, which may limit our understanding of g_m acclimation to growth conditions, particularly when the variation between treatments or studies is less than the error of estimates (Sun *et al.*, 2014a).

Populus spp., model crops in forestry characterized by high yield potential, have been the subject of numerous studies to understand the physiological response to environmental factors but research is still necessary to make assessment of effects sizes and to make generalizations (Larocque *et al.*, 2013). A general understanding of the CO_2 pathway through mesophyll and how it is affected by environmental factors would be beneficial in the effort to (i) accurately predict canopy photosynthesis under different environmental conditions, particularly under warmer and drier climate, and improve global carbon assimilation models, and (ii) effectively select more resilient and productive cultivars for wood and bioenergy. In poplar plantations, organic amendments like biosolids and pig slurry are used to increase growth rate at a low cost (Paniagua *et al.*, 2016). These amendments are rich in copper, the effect of which on photosynthetic activity, growth, and nutrient uptake has been well-documented in *Populus* spp. (Tognetti *et al.*, 2004; Borghi *et al.*, 2008; Pietrini *et al.*, 2017). In addition, poplar is a good candidate for environmental use in phytofiltration of contaminated water in agriculture lands, where copper is a major contaminant due to the large use of copper sulfate as a fungicide and in weed control (Fischerová *et al.*, 2006; Marmiroli *et al.*, 2011).

Substantial data of A–C_i response curves in the literature have been used to estimate photosynthetic parameters, not to estimate g_m, and such compiled dataset would provide a basis to make such assessments of the response of g_m to the environment. In this study, we compiled 815 A–C_i response curves from 26 datasets of different poplar species and hybrids (Table 1). Published A–C_i curve-fitting approaches differ broadly regarding the rectangularity of the hyperbola, segmentations of

Table 1. List of dataset sources used in the meta-analysis

Author	*Populus* species or hybrid parents	Number of genotypes	Treatment	Provenance of plant material	Growth Environment	Number of curves
Attia *et al.* (2015)	*P. balsamifera* L. *P. simonii* Carrière *P. balsamifera* L. × *P. simonii* Carrière	3	N/A	Canada	Growth chamber	15
Benomar *et al.* (https://doi.org/10.5061/dryad.9cnp5hqhp)	*P. maximowiczii* A. Henry × *P. balsamifera* L.	2	Water stress	Canada	Growth chamber	12
Benomar (2012)	*P. maximowiczii* A. Henry × *P. balsamifera* L. *P. balsamifera* L. × *P. trichocarpa* Torr. & A. Gray	2	Spacing and canopy level	Canada	Plantation	52
Benomar *et al.* (2019)	*P. maximowiczii* A. Henry × *P. balsamifera* L. *P. maximowiczii* A. Henry × *P. nigra* L.	2	Temperature and nitrogen	Canada	Growth chamber	23
Borghi *et al.* (2007)	*P.* × *euramericana* (*P. deltoides* W. Bartram × *P. nigra* L.) (clone Adda)	1	Copper	Italy	Growth chamber	21
Borghi *et al.* (2008)	*P. alba* L. *P.* × *Canadensis* (*P. nigra* L. × *P. deltoides* W. Bartram)	2	Copper	Italy	Growth chamber	18
Calfapietra *et al.* (2005)	*P.* × *euramericana* (*P. deltoides* W. Bartram × *P. nigra* L.)	1	Nitrogen and atmospheric CO_2 and canopy level	Italy	Plantation	60
Castagna *et al.* (2015)	*P.* × *canadensis* (*P. nigra* L. × *P. deltoides* W. Bartram) *P. deltoides* W. Bartram × *P. maximowiczii* A. Henry	2	Ozone and cadmium soil contamination	Italy	Greenhouse	16
Di Baccio *et al.* (2009)	*P.* × *euramericana* (*P. deltoides* W. Bartram × *P. nigra* L.) (clone i-214)	1	Zinc soil contamination	Italy	Growth chamber	12
Elferjani *et al.* (2016)	*P. trichocarpa* Torr. & A. Gray × *P. balsamifera* L. (clone 747215) *P. balsamifera* L. × *P. maximowiczii* A. Henry (clones 915004 and 915005) *P. maximowiczii* A. Henry × *P. balsamifera* L. (clone 915319)	4	Latitudinal gradient	Canada	Plantation	24
Li *et al.* (2013)	*P. euphratica* Oliv.	1	Ground water availability	China	In field under shelter (lysimeter)	9
Merilo *et al.* (2010)	*P. nigra* L. *P. alba* L.	2	Atmospheric CO_2 (FACE) and nitrogen and canopy level	Italy	Plantation	104
Niinemets *et al.* (1998)	*P. tremula* L.	1	Canopy level	Estonia	Natural forest stands	14
Ripullone *et al.* (2003)	*P.* × *euramericana* (*P. deltoides* W. Bartram × *P. nigra* L.) (clone i-214)	1	Nitrogen	Italy	Greenhouse	14
Ryan *et al.* (2009)	*P. deltoides* W. Bartram × *P. trichocarpa* Torr. & A. Gray	2	Ozone	United Kingdom	Greenhouse	118

Table 1. Continued

Author	*Populus* species or hybrid parents	Number of genotypes	Treatment	Provenance of plant material	Growth Environment	Number of curves
Silim *et al.* (2010)	*P. balsamifera* L.	1	Habitat and growth temperature	Canada	Greenhouse	30
Soolanayakanahally *et al.* (2009)	*P. balsamifera* L.	1	Latitudinal gradient	Canada	Greenhouse	72
Théroux-Rancourt *et al.* (https://doi.org/10.5061/dryad.7sqv9s4s0)	*P. deltoides* W. Bartram × *P. nigra* L. (clone 3570) *P. maximowiczii* A. Henry × (*P. deltoides* W. Bartram × *P. trichocarpa* Torr. & A. Gray) (clones 505372 and 505508) *P. maximowiczii* A. Henry × *P. trichocarpa* Torr. & A. Gray (clone 750361) *P. maximowiczii* A. Henry × *P. balsamifera* L. (clones 915302, 915313, 915318) (*P. deltoides* W. Bartram × *P.* nigra L.) × *P. trichocarpa* Torr. & A. Gray (clone 915508)	8	Water stress	Canada	Greenhouse	38
Théroux-Rancourt *et al.* (2014)	*Assiniboine:* [(*P.* × *'Walker':* *P. deltoides* W. Bartram × *P.* × *petrowskiana* R. I. Schrod. ex Regel) × male parent unknown] Okanese [(*P.*×'Walker') × *P.*× *petrowskiana* R. I. Schrod. ex Regel]	2	N/A	Canada	Greenhouse and growth chamber	**3**
Théroux-Rancourt *et al.* (2015)	(*P. maximowiczii* A. Henry)× (*P. deltoidesW. Bartram* × *P. trichocarpa* Torr. & A. Gray) *P. maximowiczii* A. Henry × *P. balsamifera* L. 'Walker' [*P. deltoides* W. Bartram × (*P. laurifolia Ledeb.* × *P. nigra L.*)] × *P. deltoides* W. Bartram 'Walker' × *P. petrowskyana* Schr. *P. balsamifera* L.	5	N/A	Canada	Greenhouse and growth chamber	12
Tissue and Lewis (2010)	*P. deltoides* W. Bartram	1	Phosphorous and atmospheric CO_2	Australia	Growth chamber	76
Tognetti *et al.* (https://doi.org/10.5061/dryad.w3r2280qq)	*P.* × *euramericana* (*P. nigra* L. × *P. deltoides* W. Bartram) (clone i-214)		Zinc soil contamination	Italy	Greenhouse	24
Tognetti *et al.* (2004)	*P. deltoides* W. Bartram × *P. maximowiczii* A. Henry *P.* × *euramericana* (*P. deltoides* W. Bartram × *P. nigra* L.) (clone i-214)	2	Heavy metals	Italy	Greenhouse	24
Tosens *et al.* (2012a)	*P. tremula* L.	1	Light and water stress	Estonia	Growth chamber	8
Velikova *et al.* (2011)	*P. nigra* L.	20	Nickel soil contamination	Italy	Growth chamber (climate chamber)	16
Xu *et al.* (2020)	*P.* × *euramericana* (*P. deltoides* W. Bartram × *P. nigra* L.) (cv. '74/76')	1	Nitrogen and ozone	China	Growth chamber	6

the model of photosynthesis, and determination of the transition value of CO_2 from carboxylation to electron transport (Harley *et al.*, 1992; Ethier and Livingston, 2004; Manter and Kerrigan, 2004; Dubois *et al.*, 2007; Sharkey *et al.*, 2007; Pons *et al.*, 2009; Gu *et al.*, 2010). These approaches led to different fitted values (Miao *et al.*, 2009; Sun *et al.*, 2014a). Although A–C_i curve fitting is unreliable for species with large g_m, it can provide results similar to those obtained from direct measurements for species with medium to low g_m (Niinemets *et al.*, 2005, 2006; Warren, 2006; Qiu *et al.*, 2017; Xu *et al.*, 2020). Using the compiled A–C_i response curves, we performed curve fitting using a single method (Ethier and Livingston, 2004) to alleviate the fitting method bias and to obtain uniformed estimates of g_m, maximum rate of carboxylation (V_{cmax}) and rate of electron transport (J). We further collected related variables like leaf nitrogen content, stomatal conductance, and specific leaf area (SLA) when data were available. Our main goal was to find trends in the response of mesophyll conductance to prevalent abiotic stressors and to examine the relationship between g_m and other leaf traits. We believe that a meta-analytical approach to analyse the accumulated data on the diffusion of CO_2 through the mesophyll diffusion pathway in relation to other photosynthesis-related traits provides key insights into the different controls on mesophyll conductance and into the environmental plasticity of mesophyll conductance. We aim to contribute to the efforts of improving poplar photosynthetic efficiency in poplar breeding programs, and to improve modelling of global carbon assimilation of biomass and bioenergy crops under climate change.

Materials and methods

Data collection

Data were collected by a web search in Web of Science, Scopus, and Google Scholar using the following key words: ('*Populus*' or 'poplar' or 'hybrid poplar' or 'aspen') and ('V_{cmax}' or 'maximum rate of electron transport (J_{max})' or 'mesophyll conductance'). At this step, the abstract of every item was checked to confirm the paper is actually about g_m. Then, we looked at the 'Materials and methods' section of selected papers where A–C_i response curves of *Populus* spp. were measured.

To get raw data of A–C_i response curves, we contacted the corresponding authors or co-authors of the targeted studies by e-mail and via ResearchGate. We obtained 23 datasets from published studies and three datasets from Benhomar, Tognetti and Théroux-Rancourt studies (Table 1; datasets available at Dryad Digital Repository). Collectively, they provided a total of 815 A–C_i response curves.

The total data of 72 genotypes were collected from measurements on plants growing in plantations (five studies), or under controlled conditions (greenhouse or growth chamber set-ups; 21 studies) with optimal and stressful conditions (Table 1). After compiling all A–C_i curves, the quality of the data was assessed based on the following criteria: (i) only curves with at least two points in the saturation region (J region) were retained; (ii) only fitted curves with P-value <0.05 using the method of Ethier and Livingston (2004) were retained, and consequently 65 curves that did not meet these conditions were removed; and (iii) based on the literature, g_m values in *Populus* spp. using at least two methods simultaneously never exceeded 1 mol m^{-2} s^{-1} (Singsaas *et al.*, 2004; Flexas *et al.*, 2008; Velikova *et al.*, 2011; Tosens *et al.*, 2012*a*; Théroux-Rancourt *et al.*, 2014; Momayyezi and Guy, 2017; Xu *et al.*, 2020). Then, g_m values >1 mol m^{-2} s^{-1} were considered as non-available data (94 entries), and V_{cmax} and J values were retained for further analyses.

Data subsets

To examine the effect of a given abiotic factor on g_m, we estimated that a minimum of three studies is necessary to have reliable conclusions, regardless of the genotype used, except copper for which only two studies were examined because they had been conducted under the same experimental conditions. Then, we could come up with subsets of data that focused on the same variable and performed analyses on them separately (identified in the column 'Treatment' in Table 1). Our first goal was to examine the effect of variations in these factors on g_m, light-saturated photosynthetic rate (A_{max}), g_s, J, V_{cmax}, and in a second step, the relationships between g_m and other photosynthetic characteristics (A_{max}, g_s, J, V_{cmax}). The data subsets included the following environmental factors:

- Canopy level: four studies addressed the photosynthetic activity of leaves at the bottom, middle and top of trees (Niinemets *et al.*, 1998; Calfapietra *et al.*, 2005; Merilo *et al.*, 2010; Benomar, 2012).
- Atmospheric CO_2: we examined the response of trees to elevated atmospheric CO_2 from the studies of Calfapietra *et al.* (2005), Merilo *et al.* (2010) and Tissue and Lewis (2010). We considered 370 ppm as the control treatment in the three studies, while the elevated CO_2 was 550 ppm of CO_2 for the studies of Calfapietra *et al.* (2005) and Merilo *et al.* (2010), and 700 ppm for the study of Tissue and Lewis (2010).
- Copper (Cu) stress: datasets from the studies of Borghi *et al.* (2007) and Borghi *et al.* (2008) were used to examine the response of poplar trees to contamination of the substrate with Cu. Treatments were assigned to three levels of Cu: 0 (0–0.4 μM), 20 (20–25 μM) and 75 (75–100 μM).
- Soil nitrogen (N) content: high *vs.* low soil N content treatments were reported in four studies: Ripullone *et al.* (2003), Calfapietra *et al.* (2005), Benomar *et al.* (2018) and Xu *et al.* (2020). In the study of Merilo *et al.* (2010), the authors showed that no effect of nitrogen fertilization was observed due to high background nutrient availability in the plantation site.
- Soil moisture: water status of trees was assessed and data from four studies were classified into two treatments: control (optimal watering) *vs.* water deficit (Li *et al.*, 2013; Tosens *et al.*, 2012*a*; Théroux-Rancourt (data available at Dryad Digital Repository: https://doi.org/10.5061/dryad.7sqv9s4s0); Benomar (data available at Dryad Digital Repository: https://doi.org/10.5061/dryad.9cnp5hqhp).

For Xu *et al.* (2020), we extracted data from the article (means and standard errors) and generated three replicates assuming a normal distribution using the SURVEYSELECT procedure of SAS (version 9.4; SAS Institute, Cary, NC, USA). The reason is that the authors used the same curve fitting approach (Ethier and Livingston, 2004) the we used in this meta-analysis study (Table 1).

For studies with two or more investigated factors, we considered the different levels of the factor of interest and the control level of the rest of the factors to avoid between-factor interaction effects on the results. For example, in Calfapietra *et al.* (2005), trees were subject to different levels of N and CO_2; when we focused on the effect of N, we selected trees exposed to ambient CO_2 only (control).

Curve analysis

Mesophyll conductance and photosynthetic capacity variables, V_{cmax} and J, were estimated by fitting A–C_i curve with the non-rectangular hyperbola version (Ethier and Livingston, 2004) of the biochemical model of

C_3 plants (Farquhar *et al.*, 1980). This method was calibrated for low g_m species (<0.3 mol m^{-2} s^{-1}) and its accuracy is similar to estimates using the chlorophyll fluorescence method and online carbon ^{13}C isotope discrimination (Niinemets *et al.*, 2005, 2006; Ethier *et al.*, 2006; Tomás *et al.*, 2013; Qiu *et al.*, 2017; Xu *et al.*, 2020). The model was fitted using non-linear regression techniques (Proc NLIN, SAS) following Dubois *et al.* (2007) and Sun *et al.* (2014a).

Briefly, the net assimilation rate (A_n) is given as:

$$A_n = \min\ \{A_c,\ A_j\} \tag{1}$$

with

$$A_c = V_{cmax}\frac{(C_c - \Gamma^*)}{C_c + K_c\left(1 + \frac{O}{K_o}\right)} - R_{day} \tag{2}$$

$$A_j = J\ \frac{C_c - \Gamma^*}{4\,(C_c + 2\Gamma^*)} - R_{day} \tag{3}$$

$$C_c = C_i - \frac{A_n}{g_m} \tag{4}$$

where A_c is the Rubisco-limited rate of CO_2 assimilation (μmol m^{-2} s^{-1}), A_j is the RuBP-limited rate of CO_2 assimilation (μmol m^{-2} s^{-1}), V_{cmax} is the maximum rate of carboxylation (μmol m^{-2} s^{-1}), O is the partial atmospheric pressure of O_2 (mmol mol^{-1}), Γ^* is the CO_2 compensation point in the absence of mitochondrial respiration, R_{day} is mitochondrial respiration in the light (μmol CO_2 m^{-2} s^{-1}), C_c is the chloroplast CO_2 (μmol mol^{-1}), C_i is the intercellular air space concentration of CO_2 (μmol mol^{-1}), K_c (μmol mol^{-1}) and K_o (mmol mol^{-1}) are the Michaelis–Menten constants of Rubisco for CO_2 and O_2, respectively, and J is the rate of electron transport (μmol m^{-2} s^{-1}). The values at 25 °C used for K_c, K_o, and Γ^* were 272 μmol mol^{-1}, 166 mmol mol^{-1} and 37.4 μmol mol^{-1}, respectively (Sharkey *et al.*, 2007), and their temperature dependencies were as in Sharkey *et al.* (2007).

In four datasets, measurements were carried out under a temperature that was different from the reference (25 °C). In this case, V_{cmax} and J were normalized to 25 °C using the model of Kattge and Knorr (2007), which integrates the acclimation to growth temperature. However, the actual values of V_{cmax} and J were more often significant compared with normalized values, and this was true using both ANOVA and regression analyses.

Quantitative limitations analysis

The stomatal conductance (L_s), mesophyll conductance (L_m), and biochemical (L_b) relative limitations to photosynthesis were estimated following Grassi and Magnani (2005) as modified by Tomás *et al.* (2013):

$$L_s = \frac{\left(g_{tot}/g_{sc}\right)\partial A_c/\partial C_c}{g_{tot} + \partial A_c/\partial C_c} \tag{5}$$

$$L_m = \frac{\left(g_{tot}/g_{m}\right)\partial A_c/\partial C_c}{g_{tot} + \partial A_c/\partial C_c} \tag{6}$$

$$L_b = \frac{g_{tot}}{g_{tot} + \partial A_c/\partial C_c} \tag{7}$$

where g_{tot} is the total CO_2 conductance and g_{sc} is the stomatal conductance to CO_2 (g_{sc}=g_{sw}/1.6).

$$g_{tot} = \frac{1}{\frac{1}{g_{sc}} + \frac{1}{g_m}} \tag{8}$$

$$\frac{\partial A_c}{\partial C_c} = \frac{V_{cmax}\left(\Gamma^* + k_c\left(1 + {}^{O}/_{k_o}\right)\right)}{\left(C_c + k_c\left(1 + {}^{O}/_{k_o}\right)\right)^2} \tag{9}$$

where $\frac{\partial A_c}{\partial C_c}$ is the first derivative of A_c with respect to C_c.

Factors for which A_{max} changed significantly (canopy level, soil nitrogen, and soil moisture), the absolute contribution of stomatal conductance limitation (S_L), mesophyll conductance (MC_L), and biochemical photosynthetic capacity limitation (B_L) to observed change of A_{max} were estimated following Grassi and Magnani (2005):

$$\frac{dA_{max}}{A_{max}} = S_L + MC_L + B_L = L_s\frac{dg_{sc}}{g_{sc}} + L_m\frac{dg_m}{g_m} + L_b\frac{dV_{cmax}}{V_{cmax}} \tag{10}$$

where $\frac{dA_{max}}{A_{max}}$ is the difference of A_{max} between the reference and the other treatments (within each factor) divided by A_{max} of the reference.

Statistical analyses

Data analysis assessing the effect of the environmental factors on g_m and the relationship between g_m and the other traits were carried out using SAS version 9.4.

For studies that focused on nitrogen, soil moisture, CO_2, canopy level and copper, the effect of treatments on light-saturated photosynthetic rate (A_{max}), g_m, and g_{sw} was assessed separately for each response variable, using mixed model analyses of variance of the primary data (Riley *et al.*, 2010; Mengersen *et al.*, 2013). 'Treatment' was the fixed effect while 'study' and 'genotype' nested within study were the random effects. The number of replicates was not necessarily balanced across treatments. The assumptions of normality of the residuals and homogeneity of variance were verified, and a log-transformation was made when necessary.

Results

The number of studies on mesophyll conductance has rapidly increased since 2000, and more remarkably since 2013 (Fig. 1A), suggesting a growing interest among plant ecophysiologists in understanding the role of g_m in photosynthesis. This pattern was very similar to the increase of publication number on mesophyll conductance in *Populus* spp. (Fig. 1B).

Canopy level

Light-saturated photosynthetic rate at an ambient CO_2 concentration (380–400 μmol mol^{-1}), A_{max}, significantly increased from 7.19±0.44 μmol m^{-2} s^{-1} on average at the bottom leaves to 13.15±0.45 μmol m^{-2} s^{-1} at the mid-canopy, to 16.29±0.53 μmol m^{-2} s^{-1} at the upper canopy (Fig. 2A; Supplementary Table S1). Similar to A_{max}, g_m had an ascending pattern, from the bottom (0.12±0.01 mol CO_2 m^{-2} s^{-1}) to the top of the canopy (0.24±0.02 mol m^{-2} s^{-1}) (Fig. 2C). Stomatal conductance (g_{sw}) was the lowest at the bottom canopy (0.17±0.01 mol H_2O m^{-2} s^{-1}) and then increased to 0.36±0.02 mol H_2O m^{-2} s^{-1} at the mid and upper canopy (Fig. 2B). The g_m/g_{sc} ratio was significantly greater at the upper

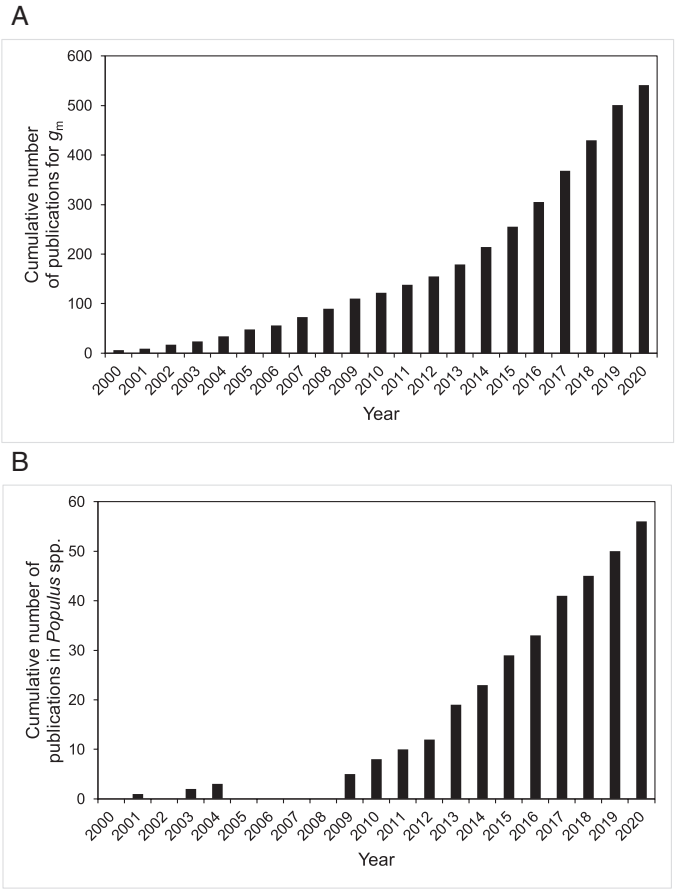

Fig. 1. Cumulative number of published studies for mesophyll conductance (g_m) between the years 2000 and 2020 (A), and cumulative number of published studies for mesophyll conductance (g_m) in *Populus* spp. between the years 2001 and 2020 (B). The number of publications was determined using keywords (e.g. g_m and *Populus*) through database search available at the Web of Science Core Collection (https://clarivate.com/webofsciencegroup/solutions/web-of-science-core-collection/).

canopy (1.17±0.11), compared with the mid-canopy leaves (0.88±0.09) and was not different everywhere else (Fig. 2D). V_{cmax} increased similarly to A_{max} and g_m from the bottom to the top of the canopy (Fig. 2E); however, SLA had an opposite trend (Fig. 2F).

Atmospheric CO_2

Increased atmospheric CO_2 had no effect on average A_{max} (14.43±0.60 μmol m^{-2} s^{-1}), g_m (0.21±0.02 mol m^{-2} s^{-1}) and g_m/g_{sc} (1.09±0.11) (Fig. 3A–C). However, average g_{sw} was higher (0.40±0.03 mol H_2O m^{-2} s^{-1}) under 'Ambient', compared with 'Elevated' CO_2 (0.32±0.02 mol H_2O m^{-2} s^{-1}) (Fig. 3B).

Copper stress

A_{max} was not affected when soil Cu concentration increased from 0 to 20 or 75 μM (9.67±0.95 μmol m^{-2} s^{-1}) (Fig. 4A). It should be noted that at the highest Cu level (75 μM), A_{max} ranged from 4 to 15 μmol m^{-2} s^{-1}. Average g_{sw} significantly decreased under medium (20 μM, 0.17±0.02 mol H_2O m^{-2} s^{-1}) and high Cu treatment (75 μM, 0.18±0.03 mol m^{-2} s^{-1}), compared with control treatment (Fig. 4B). Increasing Cu concentration in the soil did not affect g_m and the g_m/g_{sc} ratio (Fig. 4C, D).

Soil nitrogen

A_{max} was significantly greater (16.07±0.61 μmol m^{-2} s^{-1}) under high soil nitrogen (HN, 250 kg N ha^{-1} y^{-1} in field study or 20 mM for pot study) compared with low nitrogen treatment (LN, 12.93±0.65 μmol m^{-2} s^{-1}) (Fig. 5A). A high supply of nitrogen increased g_{sw} (from 0.29±0.03 in LN to 0.36±0.03 mol m^{-2} s^{-1} in HN) and g_m (from 0.19±0.02 to 0.23±0.02 to mol m^{-2} s^{-1}), but had no effect on the g_m/g_{sc} ratio (1.38±0.16 on average) (Fig. 5B–D).

Soil moisture

Average A_{max} decreased by drought (range of leaf predawn water potential under water deficit, Ψ_{leaf}=−0.7 to −0.8, soil water content=10%), dropping from 17.13±0.71 μmol m^{-2} s^{-1} to 14.62± 0.91 μmol m^{-2} s^{-1} on average with the minimum value (3.83 μmol m^{-2} s^{-1}) much lower than in watered trees (8.90 μmol m^{-2} s^{-1}) (Fig. 6A). As expected, soil moisture deficit markedly altered g_{sw}, decreasing its average value from 0.33±0.02 mol m^{-2} s^{-1} in control trees to 0.20±0.03 mol m^{-2} s^{-1} under drought conditions (Fig. 6B). Drought had the same effect on g_m, but to a lesser extent than g_{sw}. g_m decreased from 0.27±0.02 mol m^{-2} s^{-1} to 0.19±0.02 mol m^{-2} s^{-1} under soil moisture deficit (Fig. 6C). In addition, the g_m/g_{sc} ratio increased by 37% when plants were subject to drought (Fig. 6D).

Quantitative limitations

In general, photosynthetic rate was mostly limited by CO_2 diffusion (up to 75%): stomatal limitation (L_s) and mesophyll limitation (L_m) (Table 2). Biochemical limitation (L_b) of photosynthesis rate was relatively low. Higher atmospheric CO_2 decreased biochemical limitation (16.62% to 14.73%) and increased mesophyll limitation (from 41.80% to 44.28%) while stomatal limitation remained unchanged. Within the canopy, stomatal and biochemical limitations were the greatest in the upper (47.79%) and the middle (16.05%) layers of the canopy, respectively (Table 2). The mesophyll conductance limitation was higher at the middle (50.47%) and the bottom (50.85%) than at the upper part of the canopy (40.51%). The decrease of A_{max} (58.04 %) from the top, as a reference, to the bottom of the canopy (calculated with Equation 10) was mostly caused by mesophyll (absolute limitation=29.48%), followed by stomatal (19.16%) limitation and to a lesser extent by V_{cmax} (5.11%). At the middle of the canopy, the decrease of A_{max} (21.58%) was mostly due to g_m (13.15%) and to a lesser extent to V_{cmax}

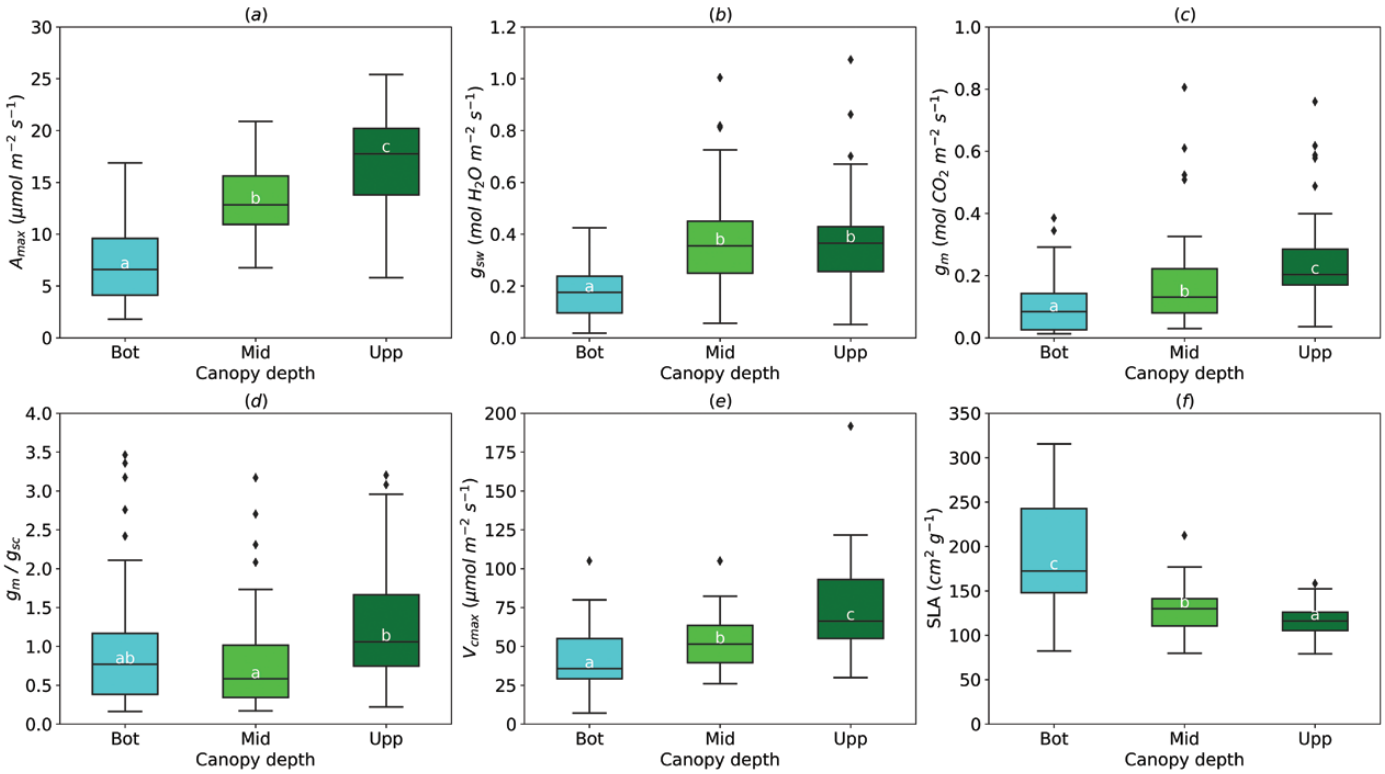

Fig. 2. Effect of the leaf position in the canopy (Bot, bottom; Mid, middle; Upp, upper) on light-saturated photosynthetic rate (A_{max}, A), stomatal conductance (g_{sw}, B), mesophyll conductance (g_m, C), g_m/g_{sc} ratio (D), maximum rate of carboxylation (V_{cmax}, E), and specific leaf area (*SLA*, F). For g_m/g_{sc} ratio, g_{sw} for water (mol H_2O m^{-2} s^{-1}) was divided by 1.6 to obtain g_{sc} (mol CO_2 m^{-2} s^{-1}). The horizontal line inside the boxes marks the median for the observations, the box ends indicate the upper (third) to lower (first) quartiles of the value ranges, and the whiskers indicate the highest and lowest observations. Means having the same letters are not significantly different at α=0.05 (number of studies=4, number of genotypes=6).

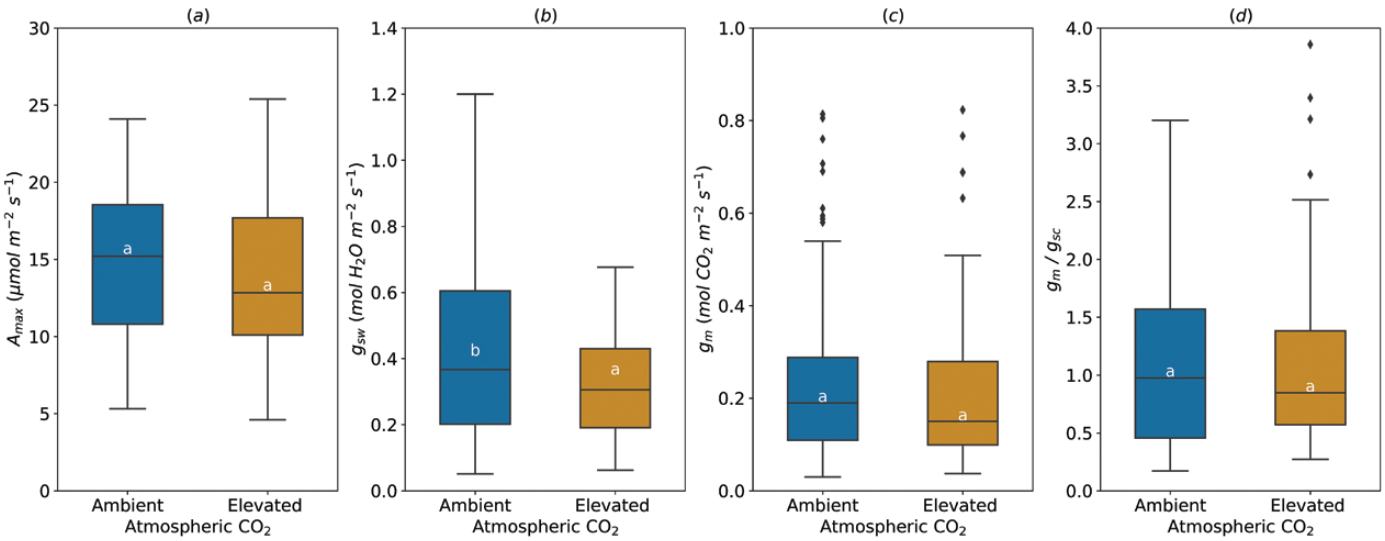

Fig. 3. Effect of the atmospheric CO_2 concentration on light-saturated photosynthetic rate (A_{max}, A), stomatal conductance (g_{sw}, B), mesophyll conductance (g_m, C), and g_m/g_{sc} ratio (D). For g_m/g_{sc} ratio, g_{sw} for water (mol H_2O m^{-2} s^{-1}) was divided by 1.6 to obtain g_{sc} (mol CO_2 m^{-2} s^{-1}). The horizontal line inside the boxes marks the median for the observations, the box ends indicate the upper (third) to lower (first) quartiles of the value ranges, and the whiskers indicate the highest and lowest observations. Means having the same letters are not significantly different at α=0.05 (number of studies=3, number of genotypes=4).

(4.74%) while the contribution of g_{sc} was marginal (2.76%). The copper stress resulted in an increase of the stomatal limitation and a decrease in mesophyll and biochemical limitations. Change in soil nitrogen did not affect the status of the limitations. The decrease of A_{max} (20.11 %) under low soil nitrogen was mostly caused by g_{sc} (9.38%) and g_m (7.58%) and to a lesser extent by V_{cmax} (1.42%). Water stress increased stomatal limitation and decreased biochemical limitation but had

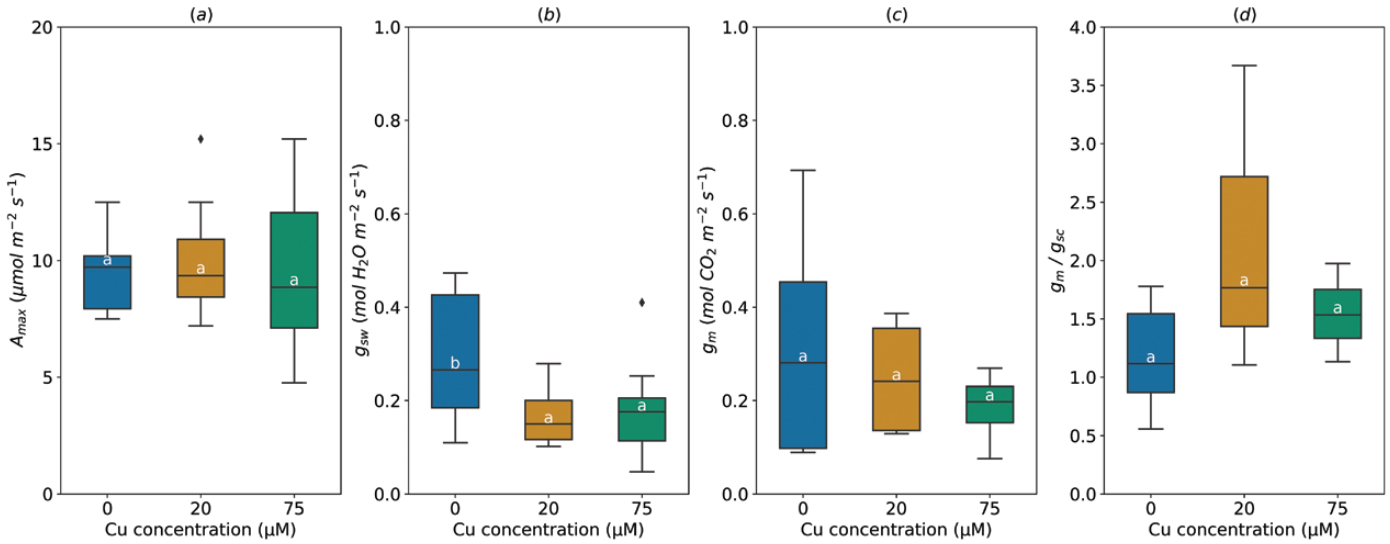

Fig. 4. Effect of the soil copper (Cu) concentration on light-saturated photosynthetic rate (A_{max}, A), stomatal conductance (g_{sw}, B), mesophyll conductance (g_m, C), and g_m/g_{sc} ratio (D). For g_m/g_s ratio, g_s for water (mol H_2O m^{-2} s^{-1}) was divided by 1.6 to obtain g_{sc} (mol CO_2 m^{-2} s^{-1}). The horizontal line inside the boxes marks the median for the observations, the box ends indicate the upper (third) to lower (first) quartiles of the value ranges, and the whiskers indicate the highest and lowest observations. Means having the same letters are not significantly different at α=0.05 (number of studies=2, number of genotypes=3).

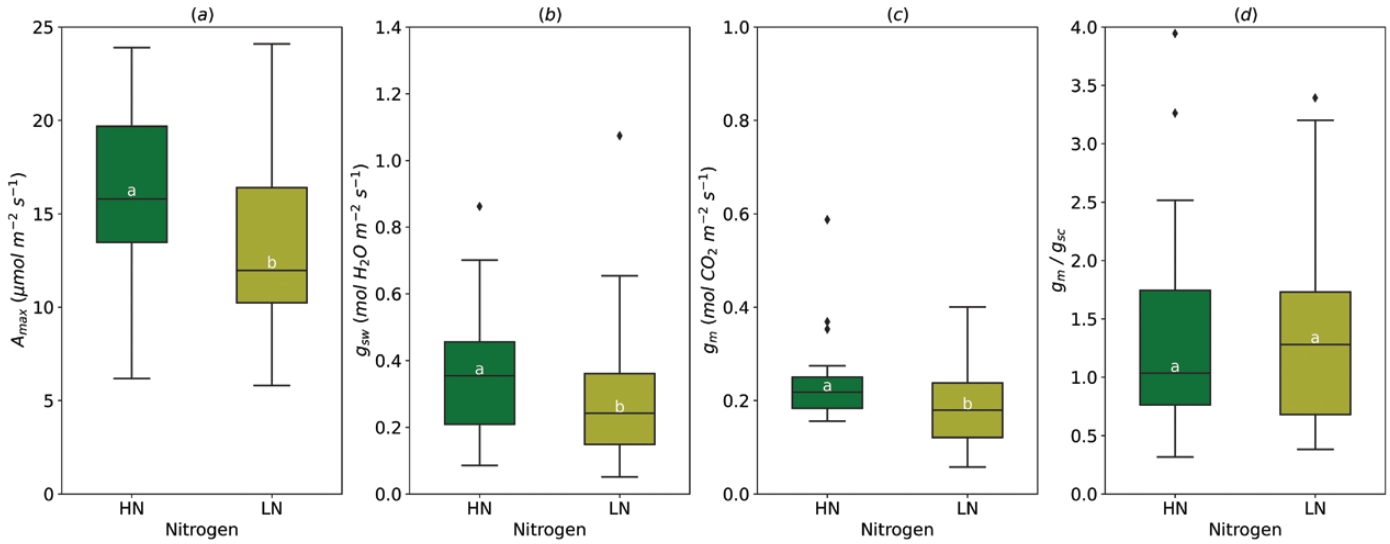

Fig. 5. Effect of the soil nitrogen content (HN, high nitrogen; LN, low nitrogen) on light-saturated photosynthetic rate (A_{max}, A), stomatal conductance (g_{sw}, B), mesophyll conductance (g_m, C), and g_m/g_{sc} ratio (D). For g_m/g_{sc} ratio, g_{sw} for water (mol H_2O m^{-2} s^{-1}) was divided by 1.6 to obtain g_{sc} (mol CO_2 m^{-2} s^{-1}). The horizontal line inside the boxes marks the median for the observations, the box ends indicate the upper (third) to lower (first) quartiles of the value ranges, and the whiskers indicate the highest and lowest observations. Means having the same letters are not significantly different at α=0.05 (number of studies=5, number of genotypes=7).

no effect on mesophyll limitation (Table 2). Therefore, the observed decrease in A_{max} (21.02%) under water deficit was mainly due to stomatal (15.22 %) and mesophyll limitation (7.64 %).

Relationship between CO_2 diffusion and photosynthetic activity

A_{max} was strongly correlated to both g_{sw} and g_m (P=0.001) and to V_{cmax} (P=0.001) over all the studies (Fig. 7A–C). Based on the collected data, g_m was significantly correlated to g_{sw} (P=0.04). However, the relationship was not linear. g_m was the highest (0.4–0.5 mmol m^{-2} s^{-1}) when g_{sw} values were intermediate (0.2–0.4 mol m^{-2} s^{-1}), and lowest at high g_{sw} values (Fig. 7E).

We found a significant negative exponential relationship between SLA and g_m (P=0.001) (Fig. 7G) based on the collected data from studies that measured SLA (n=12). Leaf nitrogen content reported by three studies showed a significant correlation between g_m and N content per area (N_{area})

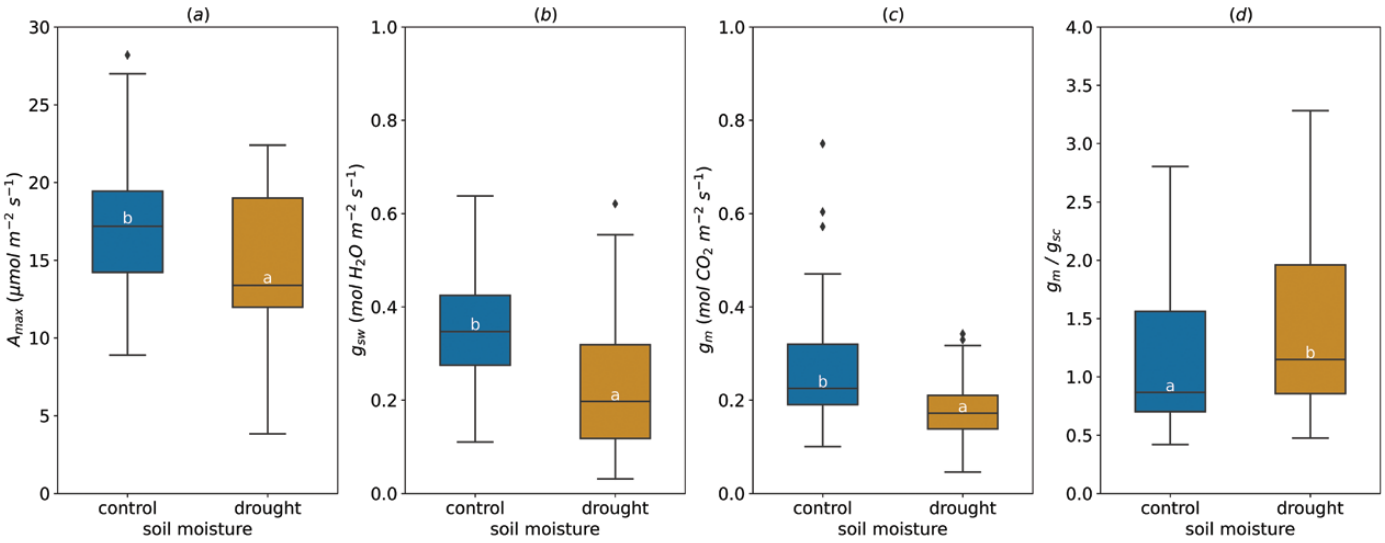

Fig. 6. Effect of the soil moisture on light-saturated photosynthetic rate (A_{max}, A), stomatal conductance (g_{sw}, B), mesophyll conductance (g_m, C), and g_m/g_{sc} ratio (D). For g_m/g_{sc} ratio, g_{sw} for water (mol H_2O m^{-2} s^{-1}) was divided by 1.6 to obtain g_{sc} (mol CO_2 m^{-2} s^{-1}). The horizontal line inside the boxes marks the median for the observations, the box ends indicate the upper (third) to lower (first) quartiles of the value ranges, and the whiskers indicate the highest and lowest observations. Means having the same letters are not significantly different at α=0.05 (number of studies=4, number of genotypes=13).

Table 2. The relative limitation (%) of stomatal conductance, mesophyll conductance, and biochemistry to photosynthesis (for each treatment, the sum of relative limitations is 100%)

Factor	Treatment	Stomatal limitation (L_s)	Mesophyll limitation (L_m)	Biochemical limitation (L_b)
Canopy level	Bottom	37.71 (2.11)	50.86 (2.68)	11.43 (1.22)
	Middle	33.46 (1.99)	50.48 (2.4)	16.06 (1.34)
	Upper	45.97 (2.18)	40.52 (1.98)	13.69 (1.09)
Atmospheric CO_2	Ambient	41.57 (2.3)	41.8 (2.27)	16.62 (1.43)
	Elevated	40.97 (1.87)	44.29 (2.04)	14.74 (1.21)
Copper stress	0 μM Cu	42.42 (6.78)	31.17 (7.38)	26.43 (7.1)
	20 μM Cu	57.88 (4.96)	25.16 (6.7)	16.96 (2.71)
	75 μM Cu	59.13 (7.58)	28.22 (6.92)	12.65 (1.29)
Soil nitrogen	High nitrogen	45.09 (2.49)	39.31 (2.07)	15.6 (1.46)
	Low nitrogen	46.02 (2.69)	39.27 (2.37)	14.71 (1.67)
Soil moisture	Control	42.47 (2.29)	38.04 (1.97)	19.49 (1.09)
	Drought	48.8 (2.78)	38.74 (2.11)	12.46 (1.25)

Data are expressed as means (SD).

(Fig. 7F). g_m increased with N_{area} until a saturation point (~0.25 mol m^{-2} s^{-1}).

Discussion

Canopy level

The scaling up of photosynthesis from leaves to the canopy and stands (using the model of Farquhar *et al.* (1980)) requires a deep understanding of within-canopy variations in leaf morpho-physiology and the main drivers of foliage acclimation to the dynamic gradient of environmental conditions (light, temperature, vapor pressure deficit (VPD) and soil moisture) (Niinemets *et al.*, 2006; Buckley and Warren, 2014; Niinemets *et al.*, 2015). Unfortunately, pieces of knowledge regarding the variation of g_m within the canopy and its mechanistic basis are scarce, in particular for *Populus* spp. This situation may explain why most global carbon cycle models remain 'g_m-lacking', with possible consequences, such as overestimation of the fertilization effect of CO_2 on global gross primary production and underestimation of water-use efficiency (WUE) and canopy gross photosynthesis under future climate (Sun *et al.*, 2014b; Knauer *et al.*, 2019).

The steep and parallel increase of g_m, A_{max}, and V_{cmax} from the bottom to the top of the canopy found here for *Populus* spp. is in agreement with the findings of Niinemets *et al.* (2006) for *Quercus ilex* L., Montpied *et al.* (2009) for *Fagus sylvatica* L., and Warren *et al.* (2003) for *Pseudotsuga menziesii* (Mirbel) Franco. A decrease of g_m from the bottom to the top of the canopy was also reported (Bögelein *et al.*, 2012; Cano *et al.*, 2013). We

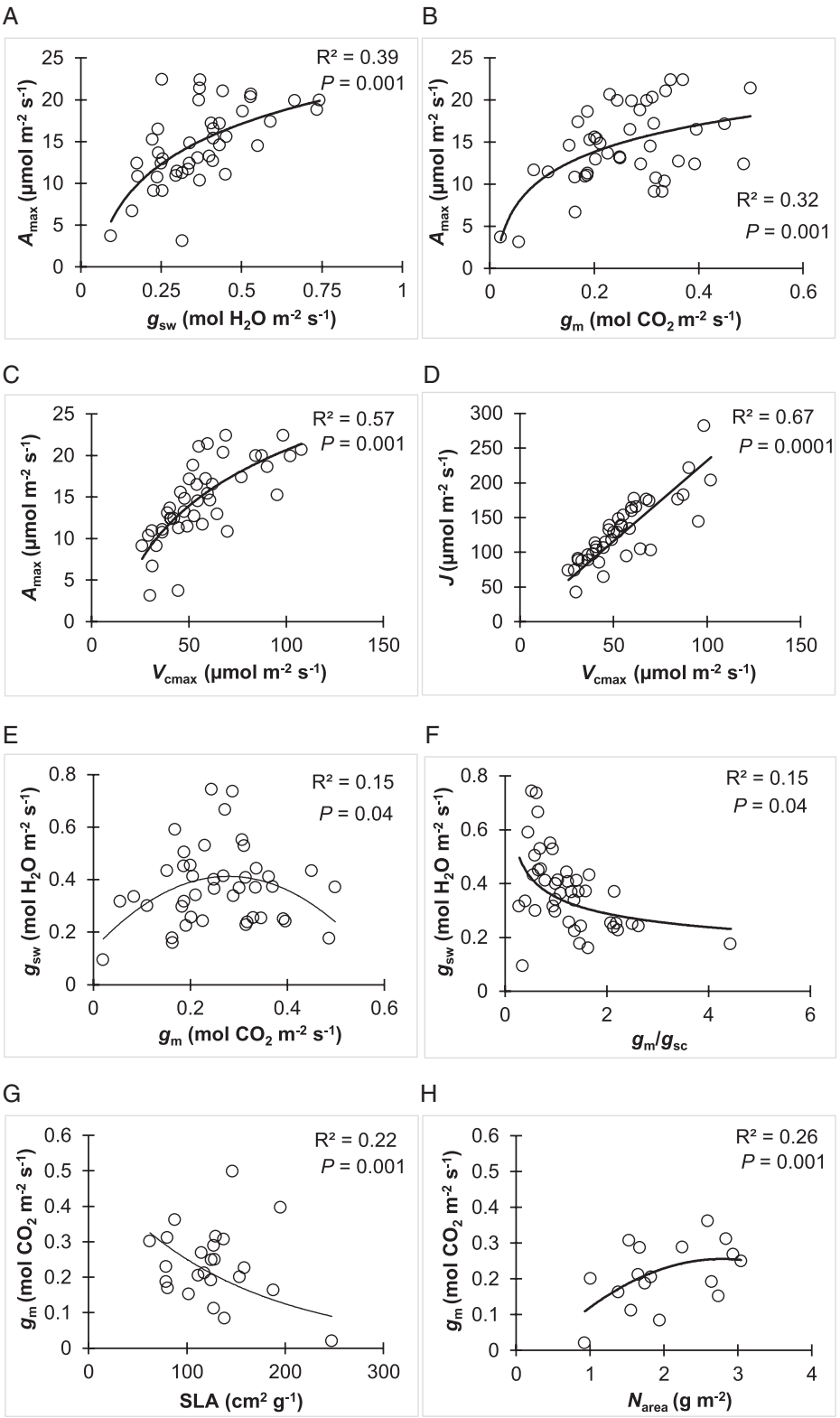

Fig. 7. Relationship between light-saturated photosynthetic rate (A_{max}), stomatal conductance (g_{sw}), mesophyll conductance (g_m), maximum rate of carboxylation (V_{cmax}), electron transport rate (J), g_m/g_{sc} ratio, specific leaf area (SLA) and per area leaf nitrogen concentration (N_{area}). For g_m/g_{sc} ratio, g_{sw} for water (mol H_2O m^{-2} s^{-1}) was divided by 1.6 to obtain g_{sc} (mol CO_2 m^{-2} s^{-1}).

observed a greater g_m limitation under shade conditions (mid and bottom of canopy), which may lead to an overestimation of canopy photosynthesis. Overall, our results highlight the need to incorporate the acclimation of g_m to light conditions along the canopy in process-based models.

We observed a significant inverse relationship between g_m and SLA, comparable to previous studies (Niinemets *et al.*, 2006; Montpied *et al.*, 2009; Tosens *et al.*, 2012*b*). This suggests that the increase in leaf thickness (lower SLA), e.g. in developing leaves and in leaves grown under higher light, may be associated with increased g_m (Tosens *et al.*, 2012*b*). Contrary to this, a positive relationship between g_m and SLA was demonstrated across *Solanum* species (Muir *et al.*, 2014), reflecting the effect of increased leaf density and mesophyll cell wall thickness on g_m. These lines of evidence collectively demonstrate the complex nature of the relationship between SLA and g_m, reflecting the circumstance that SLA is an inverse of the product of leaf thickness and density, which can respond differently to environmental drivers (Niinemets, 1999; Poorter *et al.*, 2009). The profile of g_m within the canopy observed here may be partially attributable to the morphological acclimation of *Populus* spp. foliage to light availability within the canopy. Moreover, this inverse relationship between SLA and g_m was used as an empirical model to estimate a maximum attainable g_m at different canopy layers for C_3 plants and was implemented in the Community Land Model (CLM.4.5) (Sun *et al.*, 2014b; Knauer *et al.*, 2019).

The change in morphological traits and their role in the acclimation of g_m to a vertical gradient of environmental conditions within the canopy need additional investigation. For instance, shade acclimation of leaf morphology is associated with a lower surface area of chloroplasts exposed to intercellular air spaces (S_c/S) and thicker chloroplasts (Hanba *et al.*, 2002; Niinemets *et al.*, 2006; Tosens *et al.*, 2012*b*; Peguero-Pina *et al.*, 2015). Species-specific leaf development patterns (i.e. evergreen sclerophyllous versus deciduous broadleaves) affect limitations to gas diffusion, thus determining the carbon balance of leaves (Marchi *et al.*, 2007). However, light acclimation may be species-specific and altered by water, soil nitrogen, and leaf ontogeny (Niinemets *et al.*, 2006; Tazoe *et al.*, 2009; Peguero-Pina *et al.*, 2015; Shrestha *et al.*, 2018). It is still unclear whether the g_m profile within the canopy is the result of the change in SLA.

Our results showing higher g_{sw} and g_m/g_{sc} at the top of the canopy are in disagreement with the findings of Montpied *et al.* (2009) and Bögelein *et al.* (2012), suggesting a species- and environment-specific gradient of g_m/g_s. Temperature and VPD responses of g_m and g_s are different (Cano *et al.*, 2013), resulting in different diurnal patterns of g_m and g_s. Then, the gradient of g_m/g_s ratio along the canopy may drive the WUE at the canopy level and the midday depression of photosynthetic rate regardless of the level of isohydry of clones (Cano *et al.*, 2013; Buckley and Warren, 2014; Stangl *et al.*, 2019).

Atmospheric CO_2

The response of photosynthetic capacity and diffusion of CO_2 to free-air CO_2 enrichment considerably differed between species and experimental set-ups. The decrease in A_{max} and g_{sw} in response to elevated CO_2 shown in our meta-analysis is in agreement with numerous studies on *Populus* spp. and other species (Ainsworth and Rogers, 2007; Medlyn *et al.*, 2013; DaMatta *et al.*, 2016), but is in disagreement with the findings of some other studies, e.g. Sigurdsson *et al.* (2001) and Uddling *et al.* (2009). For g_m, the effect of growth CO_2 changed among studies and some species having an intrinsic low g_m are more likely to respond to elevated CO_2 than species with high intrinsic g_m (Niinemets *et al.*, 2011). However, several studies have reported that g_m may decrease or be unresponsive to CO_2 enrichment (Singsaas *et al.*, 2004; Zhu *et al.*, 2012; Kitao *et al.*, 2015; Mizokami *et al.*, 2019). This suggests that the increase of A_{max} under elevated CO_2 cannot be attributed solely to g_m variation (Singsaas *et al.*, 2004). The absence of g_m response to elevated CO_2 complicates the research on mechanisms underlying this variation. Unlike g_m, researchers have proposed some hypotheses such as least-cost theory, nitrogen limitation, and resources investment to explain the decrease of A_{max}, V_{cmax}, and g_s under elevated CO_2 (Leakey *et al.*, 2009; Smith and Keenan, 2020).

Copper stress

Similar to our findings, g_m remained unchanged in the herbaceous plant *Silene paradoxa* L., exposed to high Cu concentration, although g_s decreased significantly (Bazihizina *et al.*, 2015). In other cases of exposure to other heavy metals, like nickel (Ni), Velikova *et al.* (2011) reported a significant decrease in chloroplast CO_2 content and mesophyll conductance in black poplar (*P. nigra* L.) exposed to 200 μM Ni under a hydroponic set-up (compared with control of 30 μM Ni). This reduction of g_m might be attributed to an alteration of leaf structure by toxic effects of high concentrations of heavy metals in mesophyll cells (Velikova *et al.*, 2011). Hermle *et al.* (2007), reported an acceleration of senescence and necrosis of mesophyll cells in *P. tremula* L. leaves exposed to Cu, Zn, Cd, and Pb at 640, 3000, 10, and 90 mg kg^{-1} soil, respectively, and a decrease of chloroplast size from the early stages of exposure. The study of Hermle *et al.* (2007) also reported the thickening of cell walls and change of their chemical composition in damaged mesophyll cells, which might have affected permeability of cell walls and diffusion of CO_2 through them. Mercury (Hg; $HgCl_2$ form) altered CO_2 diffusion through aquaporins, a membrane channel of CO_2 diffusion, in faba bean (*Vicia faba* L.) (Terashima and Ono, 2002) and significantly reduced g_m in *P. trichocarpa* Torr. & Gray. $HgCl_2$ may also decrease g_m indirectly by disrupting carbonic anhydrase activity, as reported by Momayyezi and Guy (2018), who demonstrated that carbonic

anhydrase activity is strongly associated with g_m variation in *P. trichocarpa* Torr. & Gray (Momayyezi and Guy, 2017).

Soil nitrogen

The increase of A_{max} by the enhancement of V_{cmax} in response to more available soil nitrogen has been established in the literature. However, the possible contribution of g_m to this augmentation remains unexplored for several species. Our results showed a concomitant increase of g_m with a higher supply of N. A positive correlation between the level of expression of aquaporin genes (plasma membrane intrinsic proteins and tonoplast intrinsic proteins) and g_m has been reported (Hanba *et al.*, 2004; Flexas *et al.*, 2006; Kaldenhoff *et al.*, 2008; Perez-Martin *et al.*, 2014), although it is still unclear whether this is a direct effect or a pleiotropic effect reflecting simultaneous increase in A_{max}, g_m, and g_s (Flexas *et al.*, 2012). Recent studies have demonstrated that an increase in g_m has coincided with an increase in the amount of aquaporins after fertilization (Miyazawa *et al.*, 2008b; Zhu *et al.*, 2020). The biochemical limitation to photosynthesis was relatively low (16%) and the absolute contribution of this limitation to the decrease in A_{max} under low nitrogen was much lower again (1.5%). This suggests that the limitations to photosynthesis resulting from low soil nitrogen are more attributable to CO_2 diffusion for *Populus* spp.

Soil moisture

Although many studies showed a decline of g_m in response to soil water deficit (Flexas *et al.*, 2009; Galle *et al.*, 2009; Tosens *et al.*, 2012*a*), it remains unclear if this limitation is happening within the mesophyll environment or occurs as a result of a stomatal limitation, which decreases intercellular CO_2 (C_i). Ma *et al.* (2021) reported that, across a broad range of species, g_m and g_s decline concomitantly, which has the effect of keeping the g_m/g_{sc} ratio constant for all species and between well-watered and water-stressed plants, but with variation between plant functional types. We report similar g_m/g_{sc} ratios within our soil moisture dataset. However, reports in poplar have shown that this concomitant decline is not present all the time or within the full range of g_m and g_s values observed. Théroux Rancourt *et al.* (2015) showed that, in hybrid poplar, g_m remained unchanged (~0.3 mol m^{-2} s^{-1}) following soil drying until $\Psi_{leaf} \approx -1.2$ MPa, after which g_m decreased significantly. Our results showed that although g_m/g_s increased under water deficit conditions, stomatal conductance was, in absolute term, the most important limitation to A_{max}, as reported elsewhere (Cano *et al.*, 2013). In a trial on *Quercus robur* L. and *Fraxinus angustifolia* Vahl grown in the field, Grassi and Magnani (2005) reported a concomitant decrease of both g_s and g_m in a dry year ($\Psi_{soil} \approx -1.7$ MPa), compared with a wetter year ($\Psi_{soil} \approx -0.2$ MPa). In *P. tremula* L., g_m significantly declined when Ψ_{leaf} of saplings dropped from −0.3 to −0.7 MPa due to applied osmotic stress (Tosens *et al.*, 2012*a*). Simultaneously, drought stress induced a decrease in SLA accompanied with an increase in the cell wall thickness and a decrease in the chloroplast surface area exposed to the intercellular air space per unit leaf area (Tosens *et al.*, 2012*a*). Other studies have shown that biochemical changes induced by drought stress could decrease CO_2 diffusion to carboxylation sites in the chloroplast (Miyazawa *et al.*, 2008a).

Adaptation to the local environment might be a key driver of g_m variation among taxa, similarly to other morpho-physiological traits. Interspecific and intraspecific differences in g_m from mesic versus xeric environments (*Quercus* spp. and *Eucalyptus* spp.) were reported by Zhou *et al.* (2014). Their study showed that g_m, as well as g_s, V_{cmax}, and J of species from drier regions was less sensitive to water deficit, which maintains transpiration and photosynthesis activity at higher rates under drought, compared with species from the mesic environment. Marchi *et al.* (2008) observed that structural protection of mesophyll cells had a priority over functional efficiency of photochemical mechanisms in *Olea europaea* L. (evergreen sclerophyllous) but not in *Prunus persica* L. (deciduous broadleaf), depending on age-related variation in mesophyll anatomy.

Conclusion and future directions

The present review shows that g_m in *Populus* spp. varies predictably along light gradients and that it responds to changes in soil moisture and nutrient availability, but is not affected by metal concentration and increasing atmospheric CO_2 concentration. Although metabolic processes noticeably influence the response of g_m to environmental changes, physical constraints through leaf development and ageing need to be considered in scaling photosynthesis from leaf to canopy, and in breeding programs for high WUE. Because fast-growing *Populus* spp. trees are important players in combating climate change, mitigating carbon emissions to some extent, comparisons of genotypes with different adaptations to changing environments and breeding for novel genotype–climate associations are urgently needed. This study shows that the variability of g_m in different experimental conditions offers a potential indicator for improving *Populus* spp. productivity and resilience. However, more research is yet needed, also combined with anatomical studies, to better understand the sources of variation of CO_2 diffusion through the mesophyll and their consequences on carbon assimilation and growth.

Moreover, determination of the efficiency and optimal age for early selection of fast-growing poplar clones require an understanding of the genetic control and age-based genetic correlations for traits related to g_m and growth. For that, a detailed evaluation of the genotypic control of the variances and clonal heritability of g_m is needed. Finally, the identification of molecular bases of the regulation of g_m is necessary to further refine a multi-criteria early selection approach of poplar clones dedicated to the future forestry

capable of ensuring better productivity and increased resistance to environmental stresses (frost, drought, water logging, heavy metals, heat waves, etc.).

Supplementary data

The following supplementary data are available at *JXB* online.

Table S1. Analysis of variance of the effect of different factors on photosynthesis-related traits.

Acknowledgements

This research was supported by the University of Québec in Abitibi-Témiscamingue (UQAT) as startup funds to ML. The authors acknowledge researchers who kindly provided data used in the meta-analysis, and the editor and two anonymous reviewers for their constructive comments.

Author contributions

RE and LB conceived the study, developed methodology, carried out data curation, formal analysis, investigation, data visualization, wrote original draft, and reviewed and edited the manuscript. MM contributed to data curation and visualization, and to reviewing and editing the manuscript. RT and UN contributed to investigation, methodology, and to reviewing and editing the manuscript. MM carried out funding acquisition and contributed to reviewing and editing the manuscript. RYS, GTR, TT, FR. SBG, MSL, and CC contributed to reviewing and editing the manuscript.

Conflict of interest

The authors declare that there is no conflict of interest.

Data availability

Soil moisture data from Théroux-Rancourt are available at Dryad Digital Repository (https://doi.org/10.5061/dryad.7sqv9s4s0); Benomar data are available at Dryad Digital Repository (https://doi.org/10.5061/dryad.9cnp5hqhp);Tognetti data are available at Dryad Digital Repository (https://doi.org/10.5061/dryad.w3r2280qq). All other datasets generated for this study are available from the corresponding author upon request.

References

Ainsworth EA, Rogers A. 2007. The response of photosynthesis and stomatal conductance to rising [CO_2]: mechanisms and environmental interactions. Plant, Cell & Environment **30**, 258–270.

Attia Z, Domec JC, Oren R, Way DA, Moshelion M. 2015. Growth and physiological responses of isohydric and anisohydric poplars to drought. Journal of Experimental Botany **66**, 4373–4381.

Barbour MM, Evans JR, Simonin KA, von Caemmerer S. 2016. Online CO_2 and H_2O oxygen isotope fractionation allows estimation of mesophyll conductance in C_4 plants, and reveals that mesophyll conductance decreases as leaves age in both C_4 and C_3 plants. New Phytologist **210**, 875–889.

Barbour MM, Warren CR, Farquhar GD, Forrester G, Brown H. 2010. Variability in mesophyll conductance between barley genotypes, and effects on transpiration efficiency and carbon isotope discrimination. Plant, Cell & Environment **33**, 1176–1185.

Bazihizina N, Colzi I, Giorni E, Mancuso S, Gonnelli C. 2015. Photosynthesizing on metal excess: copper differently induced changes in various photosynthetic parameters in copper tolerant and sensitive *Silene paradoxa* L. populations. Plant Science **232**, 67–76.

Benomar L. 2012. Plantation de peuplier hybride dans la région boréale du Canada: Espacement entre les arbres, déploiement mixte et modélisation éco-physiologique de l'assimilation du carbone à l'échelle de la canopée. PhD thesis, Université du Québec en Abitibi-Témiscamingue. https://depositum.uqat.ca/id/eprint/442

Benomar L. 2021. Dataset: Mesophyll conductance to CO2 in relation to drought in hybrid poplar. Dryad Digital Repository https://doi.org/10.5061/dryad.9cnp5hqhp

Benomar L, Lamhamedi MS, Pepin S, Rainville A, Lambert MC, Margolis HA, Bousquet J, Beaulieu J. 2018. Thermal acclimation of photosynthesis and respiration of southern and northern white spruce seed sources tested along a regional climatic gradient indicates limited potential to cope with temperature warming. Annals of Botany **121**, 443–457.

Benomar L, Moutaoufik MT, Elferjani R, Isabel N, DesRochers A, El Guellab A, Khlifa R, Idrissi Hassania LA. 2019. Thermal acclimation of photosynthetic activity and RuBisCO content in two hybrid poplar clones. PLoS One **14**, e0206021.

Bögelein R, Hassdenteufel M, Thomas FM, Werner W. 2012. Comparison of leaf gas exchange and stable isotope signature of water-soluble compounds along canopy gradients of co-occurring Douglas-fir and European beech. Plant, Cell & Environment **35**, 1245–1257.

Borghi M, Tognetti R, Monteforti G, Sebastiani L. 2007. Responses of *Populus* × *euramericana* (*P. deltoides* × *P. nigra*) clone Adda to increasing copper concentrations. Environmental and Experimental Botany **61**, 66–73.

Borghi M, Tognetti R, Monteforti G, Sebastiani L. 2008. Responses of two poplar species (*Populus alba* and *Populus* × *canadensis*) to high copper concentrations. Environmental and Experimental Botany **62**, 290–299.

Bown HE, Watt MS, Mason EG, Clinton PW, Whitehead D. 2009. The influence of nitrogen and phosphorus supply and genotype on mesophyll conductance limitations to photosynthesis in *Pinus radiata*. Tree Physiology **29**, 1143–1151.

Buckley TN, Warren CR. 2014. The role of mesophyll conductance in the economics of nitrogen and water use in photosynthesis. Photosynthesis Research **119**, 77–88.

Calfapietra C, Tulva I, Eensalu E, Perez M, De Angelis P, Scarascia-Mugnozza G, Kull O. 2005. Canopy profiles of photosynthetic parameters under elevated CO_2 and N fertilization in a poplar plantation. Environmental Pollution **137**, 525–535.

Cano FJ, Sánchez-Gómez D, Rodríguez-Calcerrada J, Warren CR, Gil L, Aranda I. 2013. Effects of drought on mesophyll conductance and photosynthetic limitations at different tree canopy layers. Plant, Cell & Environment **36**, 1961–1980.

Castagna A, Di Baccio D, Ranieri AM, Sebastiani L, Tognetti R. 2015. Effects of combined ozone and cadmium stresses on leaf traits in two poplar clones. Environmental Science and Pollution Research International **22**, 2064–2075.

DaMatta FM, Godoy AG, Menezes-Silva PE, Martins SC, Sanglard LM, Morais LE, Torre-Neto A, Ghini R. 2016. Sustained enhancement of photosynthesis in coffee trees grown under free-air CO_2 enrichment conditions: disentangling the contributions of stomatal, mesophyll, and biochemical limitations. Journal of Experimental Botany **67**, 341–352.

Di Baccio D, Tognetti R, Minnocci A, Sebastiani L. 2009. Responses of the *Populus* × *euramericana* clone I-214 to excess zinc: carbon assimilation, structural modifications, metal distribution and cellular localization. Environmental and Experimental Botany **67**, 153–163.

Dillaway DN, Kruger EL. 2010. Thermal acclimation of photosynthesis: a comparison of boreal and temperate tree species along a latitudinal transect. Plant, Cell & Environment **33**, 888–899.

Dubois JJ, Fiscus EL, Booker FL, Flowers MD, Reid CD. 2007. Optimizing the statistical estimation of the parameters of the Farquhar–von Caemmerer–Berry model of photosynthesis. New Phytologist **176**, 402–414.

Elferjani R, DesRochers A, Tremblay F. 2016. Plasticity of bud phenology and photosynthetic capacity in hybrid poplar plantations along a latitudinal gradient in northeastern Canada. Environmental and Experimental Botany **125**, 67–76.

Ethier GJ, Livingston NJ. 2004. On the need to incorporate sensitivity to CO_2 transfer conductance into the Farquhar–von Caemmerer–Berry leaf photosynthesis model. Plant, Cell & Environment **27**, 137–153.

Ethier GJ, Livingston NJ, Harrison DL, Black TA, Moran JA. 2006. Low stomatal and internal conductance to CO_2 versus Rubisco deactivation as determinants of the photosynthetic decline of ageing evergreen leaves. Plant, Cell & Environment **29**, 2168–2184.

Evans JR, Kaldenhoff R, Genty B, Terashima I. 2009. Resistances along the CO_2 diffusion pathway inside leaves. Journal of Experimental Botany **60**, 2235–2248.

Evans JR, Sharkey TD, Berry JA, Farquhar GD. 1986. Carbon isotope discrimination measured concurrently with gas exchange to investigate CO_2 diffusion in leaves of higher plants. Functional Plant Biology **13**, 281–292.

Farquhar GD, von Caemmerer S, Berry JA. 1980. A biochemical model of photosynthetic CO_2 assimilation in leaves of C_3 species. Planta **149**, 78–90.

Fischerová Z, Tlustos P, Száková J, Sichorová K. 2006. A comparison of phytoremediation capability of selected plant species for given trace elements. Environmental Pollution **144**, 93–100.

Flexas J, Barbour MM, Brendel O, *et al.* 2012. Mesophyll diffusion conductance to CO_2: an unappreciated central player in photosynthesis. Plant Science **193–194**, 70–84.

Flexas J, Barón M, Bota J, *et al.* 2009. Photosynthesis limitations during water stress acclimation and recovery in the drought-adapted *Vitis* hybrid Richter-110 (*V. berlandieri*×*V. rupestris*). Journal of Experimental Botany **60**, 2361–2377.

Flexas J, Díaz-Espejo A, Conesa MA, *et al.* 2016. Mesophyll conductance to CO_2 and Rubisco as targets for improving intrinsic water use efficiency in C_3 plants. Plant, Cell & Environment **39**, 965–982.

Flexas J, Ribas-Carbó M, Diaz-Espejo A, Galmés J, Medrano H. 2008. Mesophyll conductance to CO_2: current knowledge and future prospects. Plant, Cell & Environment **31**, 602–621.

Flexas J, Ribas-Carbó M, Hanson DT, Bota J, Otto B, Cifre J, McDowell N, Medrano H, Kaldenhoff R. 2006. Tobacco aquaporin NtAQP1 is involved in mesophyll conductance to CO_2 in vivo. The Plant Journal **48**, 427–439.

Flexas J, Scoffoni C, Gago J, Sack L. 2013. Leaf mesophyll conductance and leaf hydraulic conductance: an introduction to their measurement and coordination. Journal of Experimental Botany **64**, 3965–3981.

Galle A, Florez-Sarasa I, Tomas M, Pou A, Medrano H, Ribas-Carbo M, Flexas J. 2009. The role of mesophyll conductance during water stress and recovery in tobacco (*Nicotiana sylvestris*): acclimation or limitation? Journal of Experimental Botany **60**, 2379–2390.

Grassi G, Magnani F. 2005. Stomatal, mesophyll conductance and biochemical limitations to photosynthesis as affected by drought and leaf ontogeny in ash and oak trees. Plant, Cell & Environment **28**, 834–849.

Gu L, Pallardy SG, Tu K, Law BE, Wullschleger SD. 2010. Reliable estimation of biochemical parameters from C_3 leaf photosynthesis–intercellular carbon dioxide response curves. Plant, Cell & Environment **33**, 1852–1874.

Hanba YT, Kogami H, Terashima I. 2002. The effect of growth irradiance on leaf anatomy and photosynthesis in *Acer* species differing in light demand. Plant, Cell & Environment **25**, 1021–1030.

Hanba YT, Shibasaka M, Hayashi Y, Hayakawa T, Kasamo K, Terashima I, Katsuhara M. 2004. Overexpression of the barley aquaporin HvPIP2;1 increases internal CO_2 conductance and CO_2 assimilation in the leaves of transgenic rice plants. Plant and Cell Physiology **45**, 521–529.

Harley PC, Thomas RB, Reynolds JF, Strain BR. 1992. Modelling photosynthesis of cotton grown in elevated CO_2. Plant, Cell & Environment **15**, 271–282.

Hermle S, Vollenweider P, Günthardt-Goerg MS, McQuattie CJ, Matyssek R. 2007. Leaf responsiveness of *Populus tremula* and *Salix viminalis* to soil contaminated with heavy metals and acidic rainwater. Tree Physiology **27**, 1517–1531.

Kaldenhoff R, Ribas-Carbo M, Sans JF, Lovisolo C, Heckwolf M, Uehlein N. 2008. Aquaporins and plant water balance. Plant, Cell & Environment **31**, 658–666.

Kattge J, Knorr W. 2007. Temperature acclimation in a biochemical model of photosynthesis: a reanalysis of data from 36 species. Plant, Cell & Environment **30**, 1176–1190.

Kitao M, Yazaki K, Kitaoka S, Fukatsu E, Tobita H, Komatsu M, Maruyama Y, Koike T. 2015. Mesophyll conductance in leaves of Japanese white birch (*Betula platyphylla* var. *japonica*) seedlings grown under elevated CO_2 concentration and low N availability. Physiologia Plantarum **155**, 435–445.

Knauer J, Zaehle S, De Kauwe MG, Bahar NHA, Evans JR, Medlyn BE, Reichstein M, Werner C. 2019. Effects of mesophyll conductance on vegetation responses to elevated CO_2 concentrations in a land surface model. Global Change Biology **25**, 1820–1838.

Larocque GR, DesRochers A, Larchevêque M, *et al.* 2013. Research on hybrid poplars and willow species for fast-growing tree plantations: its importance for growth and yield, silviculture, policy-making and commercial applications. The Forestry Chronicle **89**, 32–41.

Leakey AD, Ainsworth EA, Bernacchi CJ, Rogers A, Long SP, Ort DR. 2009. Elevated CO_2 effects on plant carbon, nitrogen, and water relations: six important lessons from FACE. Journal of Experimental Botany **60**, 2859–2876.

Li J, Yu B, Zhao C, Nowak RS, Zhao Z, Sheng Y, Li J. 2013. Physiological and morphological responses of *Tamarix ramosissima* and *Populus euphratica* to altered groundwater availability. Tree Physiology **33**, 57–68.

Ma WT, Tcherkez G, Wang XM, Schäufele R, Schnyder H, Yang Y, Gong XY. 2021. Accounting for mesophyll conductance substantially improves ^{13}C-based estimates of intrinsic water-use efficiency. New Phytologist **229**, 1326–1338.

Manter DK, Kerrigan J. 2004. A/C_i curve analysis across a range of woody plant species: influence of regression analysis parameters and mesophyll conductance. Journal of Experimental Botany **55**, 2581–2588.

Marchi S, Guidotti D, Sebastiani L, Tognetti R. 2007. Changes in assimilation capacity during leaf development in broad-leaved *Prunus persica* and sclerophyllous *Olea europaea*. Journal of Horticultural Science & Biotechnology **82**, 69–78.

Marchi S, Tognetti R, Minnocci A, Borghi M, Sebastiani L. 2008. Variation in mesophyll anatomy and photosynthetic capacity during leaf development in a deciduous mesophyte fruit tree (*Prunus persica*) and an evergreen sclerophyllous Mediterranean shrub (*Olea europaea*). Trees **22**, 559–571.

Marmiroli M, Pietrini F, Maestri E, Zacchini M, Marmiroli N, Massacci A. 2011. Growth, physiological and molecular traits in Salicaceae trees investigated for phytoremediation of heavy metals and organics. Tree Physiology **31**, 1319–1334.

Medlyn BE, Duursma RA, De Kauwe MG, Prentice IC. 2013. The optimal stomatal response to atmospheric CO_2 concentration: alternative solutions, alternative interpretations. Agricultural and Forest Meteorology **182**, 200–203.

Mengersen K, Gurevitch J, Schmid CH. 2013. Meta-analysis of primary data. In: Koricheva, J,Gurevitch J, Mengersen K, eds. Handbook of meta-analysis in ecology and evolution. Princeton, NJ: Princeton University Press, 300–312.

Merilo E, Kaurilind E, Tulva I, Räim O, Calfapietra C, Kull O. 2010. Photosynthetic response to elevated CO_2 in poplar (POP-EUROFACE) in relation to leaf nitrogen partitioning. Baltic Forestry **16**, 162–171.

Miao Z, Xu M, Lathrop RG Jr, Wang Y. 2009. Comparison of the A–C_c curve fitting methods in determining maximum ribulose 1.5-bisphosphate carboxylase/oxygenase carboxylation rate, potential light saturated electron transport rate and leaf dark respiration. Plant, Cell & Environment **32**, 109–122.

Miyazawa SI, Yoshimura S, Shinzaki Y, Maeshima M, Miyake C. 2008*a*. Deactivation of aquaporins decreases internal conductance to CO_2 diffusion in tobacco leaves grown under long-term drought. Functional Plant Biology **35**, 553–564.

Miyazawa SI, Yoshimura S, Shinzaki Y, Maeshima M, Miyake C. 2008*b*. Relationship between mesophyll conductance to CO2 diffusion and contents of aquaporin localized at plasma membrane in tobacco plants grown under drought conditions. In: Allen JF, Gantt E, Golbeck JH, Osmond B, eds. Photosynthesis. Energy from the sun. Dordrecht: Springer, 805–808.

Mizokami Y, Sugiura D, Watanabe CKA, Betsuyaku E, Inada N, Terashima I. 2019. Elevated CO_2-induced changes in mesophyll conductance and anatomical traits in wild type and carbohydrate-metabolism mutants of Arabidopsis. Journal of Experimental Botany **70**, 4807–4818.

Momayyezi M, Guy RD. 2017. Substantial role for carbonic anhydrase in latitudinal variation in mesophyll conductance of *Populus trichocarpa* Torr. & Gray. Plant, Cell & Environment **40**, 138–149.

Momayyezi M, Guy RD. 2018. Concomitant effects of mercuric chloride on mesophyll conductance and carbonic anhydrase activity in *Populus trichocarpa* Torr. & Gray. Trees **32**, 301–309.

Montpied P, Granier A, Dreyer E. 2009. Seasonal time-course of gradients of photosynthetic capacity and mesophyll conductance to CO_2 across a beech (*Fagus sylvatica* L.) canopy. Journal of Experimental Botany **60**, 2407–2418.

Muir CD, Hangarter RP, Moyle LC, Davis PA. 2014. Morphological and anatomical determinants of mesophyll conductance in wild relatives of tomato (*Solanum* sect. *Lycopersicon*, sect. Lycopersicoides; Solanaceae). Plant, Cell & Environment **37**, 1415–1426.

Niinemets Ü. 1999. Research review. Components of leaf dry mass per area – thickness and density – alter leaf photosynthetic capacity in reverse directions in woody plants. New Phytologist **144**, 35–47.

Niinemets Ü, Cescatti A, Rodeghiero M, Tosens T. 2005. Leaf internal diffusion conductance limits photosynthesis more strongly in older leaves of Mediterranean evergreen broad-leaved species. Plant, Cell and Environment **28**, 1552–1566.

Niinemets U, Cescatti A, Rodeghiero M, Tosens T. 2006. Complex adjustments of photosynthetic potentials and internal diffusion conductance to current and previous light availabilities and leaf age in Mediterranean evergreen species *Quercus ilex*. Plant, Cell & Environment **29**, 1159–1178.

Niinemets U, Díaz-Espejo A, Flexas J, Galmés J, Warren CR. 2009. Role of mesophyll diffusion conductance in constraining potential photosynthetic productivity in the field. Journal of Experimental Botany **60**, 2249–2270.

Niinemets U, Flexas J, Peñuelas J. 2011. Evergreens favored by higher responsiveness to increased CO_2. Trends in Ecology & Evolution **26**, 136–142.

Niinemets Ü, Keenan TF, Hallik L. 2015. A worldwide analysis of within-canopy variations in leaf structural, chemical and physiological traits across plant functional types. New Phytologist **205**, 973–993.

Niinemets U, Kull O, Tenhunen JD. 1998. An analysis of light effects on foliar morphology, physiology, and light interception in temperate deciduous woody species of contrasting shade tolerance. Tree Physiology **18**, 681–696.

Paniagua S, Escudero L, Escapa C, Coimbra RN, Otero M, Calvo LF. 2016. Effect of waste organic amendments on *Populus* sp. biomass production and thermal characteristics. Renewable Energy **94**, 166–174.

Peguero-Pina JJ, Sancho-Knapik D, Flexas J, Galmés J, Niinemets Ü, Gil-Pelegrín E. 2015. Light acclimation of photosynthesis in two closely related firs (*Abies pinsapo* Boiss. and *Abies alba* Mill.): the role of leaf anatomy and mesophyll conductance to CO_2. Tree Physiology **36**, 300–310.

Perez-Martin A, Michelazzo C, Torres-Ruiz JM, Flexas J, Fernández JE, Sebastiani L, Diaz-Espejo A. 2014. Regulation of photosynthesis and stomatal and mesophyll conductance under water stress and recovery in olive trees: correlation with gene expression of carbonic anhydrase and aquaporins. Journal of Experimental Botany **65**, 3143–3156.

Pietrini F, Di Baccio D, Iori V, Veliksar S, Lemanova N, Juškaitė L, Maruška A, Zacchini M. 2017. Investigation on metal tolerance and phytoremoval activity in the poplar hybrid clone "Monviso" under Cu-spiked water: potential use for wastewater treatment. The Science of the Total Environment **592**, 412–418.

Pons TL, Flexas J, von Caemmerer S, Evans JR, Genty B, Ribas-Carbo M, Brugnoli E. 2009. Estimating mesophyll conductance to CO_2: methodology, potential errors, and recommendations. Journal of Experimental Botany **60**, 2217–2234.

Poorter H, Niinemets U, Poorter L, Wright IJ, Villar R. 2009. Causes and consequences of variation in leaf mass per area (LMA): a meta-analysis. New Phytologist **182**, 565–588.

Qiu C, Ethier G, Pepin S, Dubé P, Desjardins Y, Gosselin A. 2017. Persistent negative temperature response of mesophyll conductance in red raspberry (*Rubus idaeus* L.) leaves under both high and low vapour pressure deficits: a role for abscisic acid? Plant, Cell & Environment **40**, 1940–1959.

Riley RD, Lambert PC, Abo-Zaid G. 2010. Meta-analysis of individual participant data: rationale, conduct, and reporting. British Medical Journal **340**, c221.

Ripullone F, Grassi G, Lauteri M, Borghetti M. 2003. Photosynthesis–nitrogen relationships: interpretation of different patterns between *Pseudotsuga menziesii* and *Populus* × *euroamericana* in a mini-stand experiment. Tree Physiology **23**, 137–144.

Ryan A, Cojocariu C, Possell M, Davies WJ, Hewitt CN. 2009. Defining hybrid poplar (*Populus deltoides* × *Populus trichocarpa*) tolerance to ozone: identifying key parameters. Plant, Cell & Environment **32**, 31–45.

Sharkey TD, Bernacchi CJ, Farquhar GD, Singsaas EL. 2007. Fitting photosynthetic carbon dioxide response curves for C_3 leaves. Plant, Cell & Environment **30**, 1035–1040.

Shrestha A, Buckley TN, Lockhart EL, Barbour MM. 2018. The response of mesophyll conductance to short- and long-term environmental conditions in chickpea genotypes. AoB Plants **11**, ply073.

Sigurdsson BD, Thorgeirsson H, Linder S. 2001. Growth and dry-matter partitioning of young *Populus trichocarpa* in response to carbon dioxide concentration and mineral nutrient availability. Tree Physiology **21**, 941–950.

Silim SN, Ryan N, Kubien DS. 2010. Temperature responses of photosynthesis and respiration in *Populus balsamifera* L.: acclimation versus adaptation. Photosynthesis Research **104**, 19–30.

Singsaas EL, Ort DR, Delucia EH. 2004. Elevated CO_2 effects on mesophyll conductance and its consequences for interpreting photosynthetic physiology. Plant, Cell & Environment **27**, 41–50.

Smith NG, Keenan TF. 2020. Mechanisms underlying leaf photosynthetic acclimation to warming and elevated CO_2 as inferred from least-cost optimality theory. Global Change Biology **26**, 5202–5216.

Soolanayakanahally RY, Guy RD, Silim SN, Drewes EC, Schroeder WR. 2009. Enhanced assimilation rate and water use efficiency with latitude through increased photosynthetic capacity and internal conductance in balsam poplar (*Populus balsamifera* L.). Plant, Cell & Environment **32**, 1821–1832.

Stangl ZR, Tarvainen L, Wallin G, Ubierna N, Räntfors M, Marshall JD. 2019. Diurnal variation in mesophyll conductance and its influence on modelled water-use efficiency in a mature boreal *Pinus sylvestris* stand. Photosynthesis Research **141**, 53–63.

Sun J, Feng Z, Leakey AD, Zhu X, Bernacchi CJ, Ort DR. 2014*a*. Inconsistency of mesophyll conductance estimate causes the inconsistency for the estimates of maximum rate of Rubisco carboxylation among the linear, rectangular and non-rectangular hyperbola biochemical models of leaf photosynthesis—a case study of CO_2 enrichment and leaf aging effects in soybean. Plant Science **226**, 49–60.

Sun Y, Gu L, Dickinson RE, Norby RJ, Pallardy SG, Hoffman FM. 2014*b*. Impact of mesophyll diffusion on estimated global land CO_2

fertilization. Proceedings of the National Academy of Sciences, USA **111**, 15774–15779.

Tazoe Y, von Caemmerer S, Badger MR, Evans JR. 2009. Light and CO_2 do not affect the mesophyll conductance to CO_2 diffusion in wheat leaves. Journal of Experimental Botany **60**, 2291–2301.

Terashima I, Ono K. 2002. Effects of $HgCl_2$ on CO_2 dependence of leaf photosynthesis: evidence indicating involvement of aquaporins in CO_2 diffusion across the plasma membrane. Plant and Cell Physiology **43**, 70–78.

Théroux-Rancourt G. 2021. Dataset: Mesophyll conductance acclimation to water stress in hybrid poplar. Dryad Digital Repository, https://doi.org/10.5061/dryad.7sqv9s4s0

Théroux-Rancourt G, Éthier G, Pepin S. 2014. Threshold response of mesophyll CO_2 conductance to leaf hydraulics in highly transpiring hybrid poplar clones exposed to soil drying. Journal of Experimental Botany **65**, 741–753.

Théroux Rancourt G, Éthier G, Pepin S. 2015. Greater efficiency of water use in poplar clones having a delayed response of mesophyll conductance to drought. Tree Physiology **35**, 172–184.

Tissue DT, Lewis JD. 2010. Photosynthetic responses of cottonwood seedlings grown in glacial through future atmospheric [CO_2] vary with phosphorus supply. Tree Physiology **30**, 1361–1372.

Tognetti R. 2021. Dataset: Physiological response of Populus × euramericana clone to soil zinc (Zn). Dryad Digital Repository https://doi.org/10.5061/dryad.w3r2280qq

Tognetti R, Sebastiani L, Minnocci A. 2004. Gas exchange and foliage characteristics of two poplar clones grown in soil amended with industrial waste. Tree Physiology **24**, 75–82.

Tomás M, Flexas J, Copolovici L, Galmés J, Hallik L, Medrano H, Ribas-Carbó M, Tosens T, Vislap V, Niinemets Ü. 2013. Importance of leaf anatomy in determining mesophyll diffusion conductance to CO_2 across species: quantitative limitations and scaling up by models. Journal of Experimental Botany **64**, 2269–2281.

Tosens T, Laanisto L. 2018. Mesophyll conductance and accurate photosynthetic carbon gain calculations. Journal of Experimental Botany **69**, 5315–5318.

Tosens T, Niinemets U, Vislap V, Eichelmann H, Castro Díez P. 2012*a*. Developmental changes in mesophyll diffusion conductance and photosynthetic capacity under different light and water availabilities in *Populus tremula*: how structure constrains function. Plant, Cell & Environment **35**, 839–856.

Tosens T, Niinemets Ü, Westoby M, Wright IJ. 2012*b*. Anatomical basis of variation in mesophyll resistance in eastern Australian sclerophylls: news of a long and winding path. Journal of Experimental Botany **63**, 5105–5119.

Uddling J, Teclaw RM, Pregitzer KS, Ellsworth DS. 2009. Leaf and canopy conductance in aspen and aspen-birch forests under free-air enrichment of carbon dioxide and ozone. Tree Physiology **29**, 1367–1380.

Velikova V, Tsonev T, Loreto F, Centritto M. 2011. Changes in photosynthesis, mesophyll conductance to CO_2, and isoprenoid emissions in *Populus nigra* plants exposed to excess nickel. Environmental Pollution **159**, 1058–1066.

Warren CR. 2004. The photosynthetic limitation posed by internal conductance to CO_2 movement is increased by nutrient supply. Journal of Experimental Botany **55**, 2313–2321.

Warren C. 2006. Estimating the internal conductance to CO_2 movement. Functional Plant Biology **33**, 431–442.

Warren CR. 2008. Does growth temperature affect the temperature responses of photosynthesis and internal conductance to CO_2? A test with *Eucalyptus regnans*. Tree Physiology **28**, 11–19.

Warren CR, Ethier GJ, Livingston NJ, Grant NJ, Turpin DH, Harrison DL, Black TA. 2003. Transfer conductance in second growth Douglas-fir (*Pseudotsuga menziesii* (Mirb.) Franco) canopies. Plant, Cell & Environment **26**, 1215–1227.

Xiong D, Flexas J, Yu T, Peng S, Huang J. 2017. Leaf anatomy mediates coordination of leaf hydraulic conductance and mesophyll conductance to CO_2 in *Oryza*. New Phytologist **213**, 572–583.

Xu Y, Shang B, Feng Z, Tarvainen L. 2020. Effect of elevated ozone, nitrogen availability and mesophyll conductance on the temperature responses of leaf photosynthetic parameters in poplar. Tree Physiology **40**, 484–497.

Zhou S, Medlyn B, Sabaté S, Sperlich D, Prentice IC. 2014. Short-term water stress impacts on stomatal, mesophyll and biochemical limitations to photosynthesis differ consistently among tree species from contrasting climates. Tree Physiology **34**, 1035–1046.

Zhu C, Ziska L, Zhu J, Zeng Q, Xie Z, Tang H, Jia X, Hasegawa T. 2012. The temporal and species dynamics of photosynthetic acclimation in flag leaves of rice (*Oryza sativa*) and wheat (*Triticum aestivum*) under elevated carbon dioxide. Physiologia Plantarum **145**, 395–405.

Zhu K, Wang A, Wu J, Yuan F, Guan D, Jin C, Zhang Y, Gong C. 2020. Effects of nitrogen additions on mesophyll and stomatal conductance in Manchurian ash and Mongolian oak. Scientific Reports **10**, 10038.